STUDIA UBB CHEMIA, LIX, 1, 2014 (p. 63-78)
(RECOMMENDED CITATION)

CORROSION BEHAVIOR OF Zn-Ni COATINGS ELECTRODEPOSITED IN PULSED CURRENT AND MAGNETIC FIELD ON DIFFERENT SUBSTRATES BY ELECTROCHEMICAL IMPEDANCE SPECTROSCOPY TECHNIQUES

MIHAIL CHIRA[a,*], HORATIU VERMESAN[a], VASILE RUS[a], ERNEST GRUNWALD[b]

ABSTRACT. The electrodeposition of Zn-Ni alloy was performed on different substrates and by different deposition techniques. The corrosion behavior was investigated in 1% NaCl electrolyte by potentiodynamic and electrochemical impedance spectroscopy. The corrosion resistance of the coatings depends on the deposition technique and substrate used.

Keywords: *electrodeposition, pulsed current, magnetic field, boron nitride, zinc-nickel, silicon dioxide*

INTRODUCTION

Due to the environmental protection regulations and extension of the corrosion-resistance demands for products, the automotive, machine parts, electronic, electrochemical, computers and telecommunications industries have been constrained to invest in research and development of new technologies to improve the physical-mechanical properties and corrosion resistance of iron based products, coated with suitable alloys at low cost. [1]

Zn-Ni deposits in automotive industry, especially on the car body [2], show a good behavior to pitting corrosion caused by salt and dirt that remain for long time in the hidden areas of the profiled parts. Zn-Ni alloys that contain 10-15% Ni have higher corrosion resistance [3] compared to other coatings.

[a] *Technical University of Cluj-Napoca, Romania, Departament of Materials Engineering Technical University, 103-105, B.dul Muncii, 400641 Cluj-Napoca, Romania*
[b] *SC BETAK SA Bistrita, Romania*
** Corresponding author: mihai2706@yahoo.com*

Zn-Ni alloy coatings can be electroplated on high grade alloyed and unalloyed steels, with mechanical strength up to 2100 Nmm^{-2}; however, their corrosion resistance depends on the environment.

Electroplated coatings have a micro and macroscopic structure depending on the electrolyte and the bath operating parameters. Unlike other electroplated metal coatings, Zn-Ni coatings are uniform, elastic, clean, aesthetically pleasant and obtainable at finely adjustable thickness, according to the environment in which they operate [3,4].

Physicochemical properties of Zn-Ni electrodeposited coatings depend mainly on the microstructure, phase composition and structural parameters [3].

Electrodeposition of Zn-Ni alloy is mostly studied for its corrosion protection properties. The study of the magnetic field effects on this electrodeposited alloy is interesting because of the absence of magnetic characteristics, unlike magnetic alloys such as Fe-Ni and Co-Fe [15].

Several phases are identified and from the experimental data it can be concluded that atomic nickel remains in the same ratio, the magnetic field acting as a leveling agent and leading to the formation of a uniform coating by reducing roughness and grain size. XRD diagrams show that the change on magnetic field alters the structure of the Zn deposit and the Zn-Ni alloy [6].

Pulsed current electrodeposition is an alternative technique for obtaining thin films and allows the incorporation of composite particles in high concentration and the control of the deposit (film composition, thickness up to atomic level, deposit uniformity and deposited layer roughness) by adjusting amplitude and pulse width.

Pulsed current electrodeposition influences the structure and morphology of nano-composites, the average size of crystallites due to current density and growth mechanism [7].

Electrochemical impedance spectroscopy (EIS) was used for the study of the corrosion behavior of deposited coatings, as it provides information regarding electrode capacity, charge transfer kinetics and reaction mechanism [16].

The aim of this work is to study the corrosion behavior of Zn-Ni coatings electrodeposited in pulsed current and magnetic field on different substrates and to compare this behavior with that of conventional electrodeposition.

RESULTS AND DISSCUSIONS

Potentiodynamic polarization testing

Figures 1, 2 and 3 show the potentiodynamic Tafel slopes.

The following notations will be used further on:

Table 1. Notations of the samples used in the paper.

Sample notation	Method of obtaining
ZnNi	the sample obtained by conventional electrodeposition of ZnNi alloy on steel substrate
ZnNi + f	the sample obtained by electrodeposition in pulsed current of ZnNi alloy on steel substrate
ZnNi + bp	the sample obtained by electrodeposition in a magnetic field of the ZnNi alloy on steel substrate
ZnNi + bp + f	the sample obtained by electrodeposition in pulsed current and in magnetic field of the ZnNi alloy on steel substrate
Si + ZnNi	the sample obtained by conventional electrodeposition of the ZnNi alloy on steel substrate / silicon dioxide
Si + ZnNi + f	the sample obtained by electrodeposition in pulsed current of ZnNi alloy on steel substrate / silicon dioxide
Si + ZnNi + bp	the sample obtained by electrodeposition in a magnetic field of the ZnNi alloy on steel substrate / silicon dioxide
Si + ZnNi + bp + f	the sample obtained by electrodeposition in pulsed current and in magnetic field of the ZnNi alloy on steel substrate / silicon dioxide
Si + B + ZnNi	the sample obtained by conventional electrodeposition of the ZnNi alloy on steel substrate / silicon dioxide / boron nitride
Si + B + ZnNi + f	the sample obtained by electrodeposition in pulsed current of ZnNi alloy on steel substrate / silicon dioxide / boron nitride
Si + B + ZnNi + bp	the sample obtained by electrodeposition in a magnetic field of the ZnNi alloy on steel substrate / silicon dioxide / boron nitride
Si + B + ZnNi + bp + f	the sample obtained by electrodeposition in pulsed current and in magnetic field of the ZnNi alloy on steel substrate / silicon dioxide / boron nitride

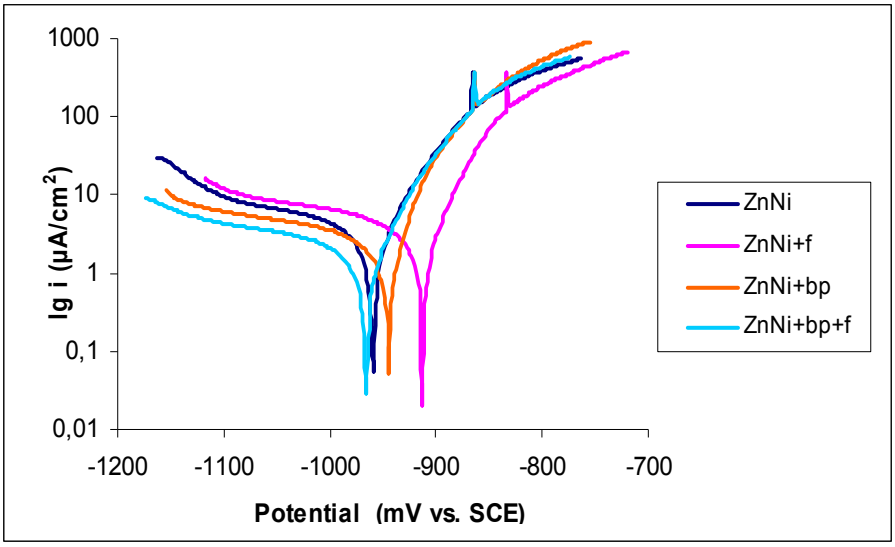

Figure 1. Polarization slopes for Zn-Ni coatings (steel substrate electroplated by the four methods) in 1% NaCl electrolyte.

Electrochemical parameters corresponding to Figure 1 are given in Table 2.

Due to the fact that the Zn-Ni alloy tends to passivate the cathodic slopes obtained in all experiments do not present a valid Tafel slope. As a result, the corrosion current density was determined using only the anodic slopes. This may generate a degree of imprecision vis-à-vis corrosion rate estimated in these conditions. However, it could perform a comparison between the behaviors of various layers. Parameters obtained as a result of the investigation of the corrosion tests are presented in Table 2.

Table 2. Corrosion rate of Zn-Ni coatings (steel substrate electroplated by the four methods) in 1% NaCl electrolyte at 25 ± 1°C.

SAMPLE	β_a [mV/decade]	β_c [mV/decade]	R_p [kΩcm^2]	E(i=0) [mV]	I_{cor} [μA/cm^2]
Zn-Ni	61.7	-416.9	5.60	-960	3.951
Zn-Ni + f	43.5	-192.3	5.97	-917.7	2.743
Zn-Ni + bp	44.0	-430.1	8.17	-950.2	2.504
Zn-Ni +bp+f	54.0	-385.2	11.24	-970.9	2.027

It was observed that Zn-Ni coatings electrodeposited in pulsed current and those in pulsed current combined with magnetic field, show lower current densities compared to the other samples. Also the anodic and cathodic Tafel slopes for the sample obtained by electrodeposition in pulsed current is lower than that of other samples. This finding indicates that the Zn-Ni coating electrodeposited in pulsed current has a higher activation energy corresponding to dissolution than that of other samples. In other words, it can be seen that the corrosion current density is two times lower compared to the one of the sample obtained by conventional electrodeposition.

The diagram and quantitative data for the samples obtained by electrodeposition of Zn-Ni coating on steel substrate / SiO_2 using the four coating techniques are shown in Figure 2 respectively Table 3.

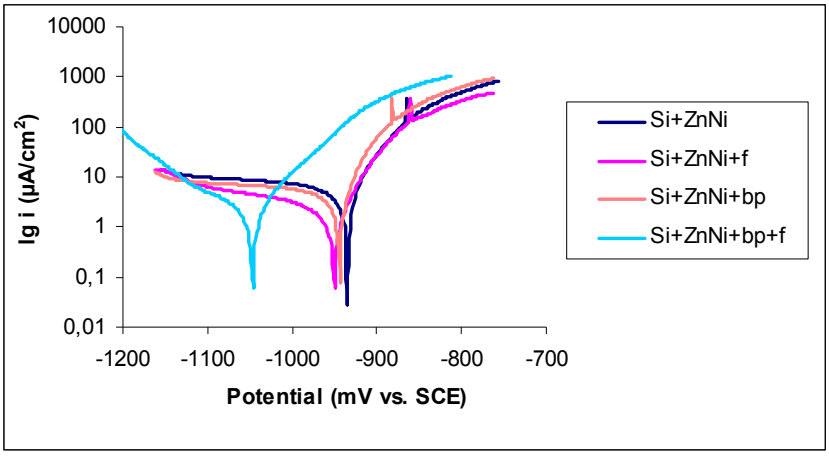

Figure 2. Polarization curves for Zn-Ni coatings (electroplated on steel substrate / SiO_2 using the four coating techniques) in 1% NaCl electrolyte.

Table 3. Corrosion rate of Zn-Ni coatings (electroplated on steel substrate / SiO_2 using the four coating techniques) in 1% NaCl electrolyte at 25 ± 1°C

SAMPLE	β_a [mV/decade]	β_c [mV/decade]	R_p [kΩcm^2]	E(i=0) [mV]	I_{cor} [μA/cm^2]
Si+ Zn-Ni	51.5	-681.7	3.75	-940.8	5.971
Si+ Zn-Ni +f	41.1	-175.1	7.03	-955.7	1.625
Si+ Zn-Ni + bp	39.2	-556.6	4.25	-950	4.601
Si+ZnNi+bp+f	48.1	-105.8	7.78	-1051.6	1.501

Analyzing the Tafel slopes (figure 2) and data shown in Table 3 it can be seen that the current densities for the samples obtained by electrodeposition of Zn-Ni coatings in pulsed current and magnetic field, were lower compared to those obtained for other samples. Also the anodic and cathodic Tafel slopes

are lower than those of other samples. This finding shows that the Zn-Ni coating electrodeposited in pulsed current and magnetic field has a higher activation energy corresponding to the dissolution compared to the other samples. The corrosion current density of sample obtained in pulsed current and magnetic field is approximately seven times lower than that of the sample obtained by conventional electrodeposition, although corrosion potential has more negative values (thermodynamic corrosion possibility) yet the kinetic factors of the developing oxide film reduce the corrosion rate and i_{cor} = 1.501 μA/cm^2.

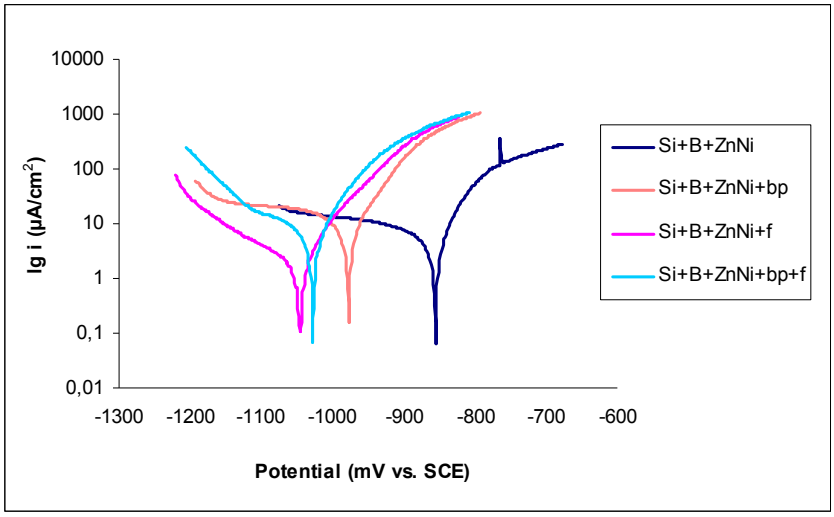

Figure 3. Polarization curves for Zn-Ni coatings (electrodeposited on steel substrate / SiO_2 / BN using the four coating techniques) in 1% NaCl electrolyte.

The diagram and quantitative data for the samples obtained by electrodeposition of Zn-Ni on steel substrate/SiO_2/BN using the four coating techniques are shown in Figure 3 and Table 4, respectively.

Table 4. Corrosion rate of Zn-Ni coatings (electroplated on steel substrate / SiO_2 / BN using the four coating techniques) in 1% NaCl electrolyte at 25 ± 1°C

SAMPLE	β_a [mV/decade]	β_c [mV/decade]	R_p [kΩcm^2]	E(i=0) [mV]	I_{cor} [μA/cm^2]
Si+B+Zn-Ni	62.3	-427.8	3.42	-860.7	6.749
Si+B+Zn-Ni+f	56.3	-157.8	8.04	-1050.7	1.886
Si+B+Zn-Ni+bp	54.2	-117.7	1.94	-982.2	6.313
Si+B+Zn-Ni+bp+f	52.2	-114.0	2.58	-1032.5	4.940

As seen in Table 4, the sample obtained by electrodeposition of Zn-Ni in pulsed current (Si + B + Zn-Ni + f) shows a lower current density compared to the other samples, and the anodic and cathode Tafel slopes are lower compared to the samples obtained by conventional electrodeposition. This finding indicates that Zn-Ni coating electrodeposited in pulsed current shows a higher activation energy corresponding to dissolution compared to that of the other samples. Corrosion current density for the sample obtained in pulsed current is about 2.6 times smaller than that of the sample obtained by conventional electrodeposition.

By grouping in Table 5 the best data results in terms of corrosion resistance for the three sets of samples, certain conclusions can be drawn.

Table 5. Corrosion rate of Zn-Ni coatings (electroplated on steel / SiO_2 and on steel / SiO_2 / BN substrates using the four coating techniques) in 1% NaCl electrolyte at 25 ± 1°C

SAMPLE	β_a [mV/decade]	β_c [mV/decade]	R_p [kΩcm^2]	E(i=0) [mV]	I_{cor} [μA/cm^2]
Zn-Ni	61.7	-416.9	5.60	-964.5	3.951
Si+ ZnNi+bp+f	48.1	-105.8	7.78	-1051.6	1.501
Si+B+Zn-Ni+f	56.3	-157.8	8.04	-1050.7	1.886

The data in Table 5 show that the corrosion current density of the (Si + Zn-Ni + bp + f) sample is lower compared to the (Si + B + Zn-Ni + f) sample, which in turn is lower compared to the Zn-Ni sample. Also the anodic and cathodic Tafel slopes for the (Si + Zn-Ni + bp + f) sample are smaller compared to the other samples, which indicates that the (Si + Zn-Ni + bp + f) sample has higher zinc dissolution activation energy, and thus has a better corrosion resistance. Although the polarization resistances for the three samples have similar value, the corrosion rates are different. It can be concluded that the corrosion resistance of the Zn-Ni coatings studied depend on the electrodeposition technique used, and on the substrate composition, the sample obtained by electrodeposition of Zn-Ni alloy on the steel substrate/SiO_2 in pulsed current and magnetic field showing the best corrosion resistance.

Electrochemical impedance spectroscopy testing

Nyquist diagrams for the samples obtained by electrodeposition of Zn-Ni alloy on steel substrate, on steel/SiO_2, and on steel/SiO_2/BN are shown in Figure 4, 5 and 6.

The shapes of the Nyquist impedance spectra for the three samples are similar and are characterized by a loop at high frequencies, followed by an ascending line at low frequencies. This shows that the corrosion process is controlled by both the charge transfer and the diffusion; the semicircular loops indicating the charge transfer.

The semicircles diameter is associated with the coating polarization resistance R_p and corresponds with the corrosion rate.

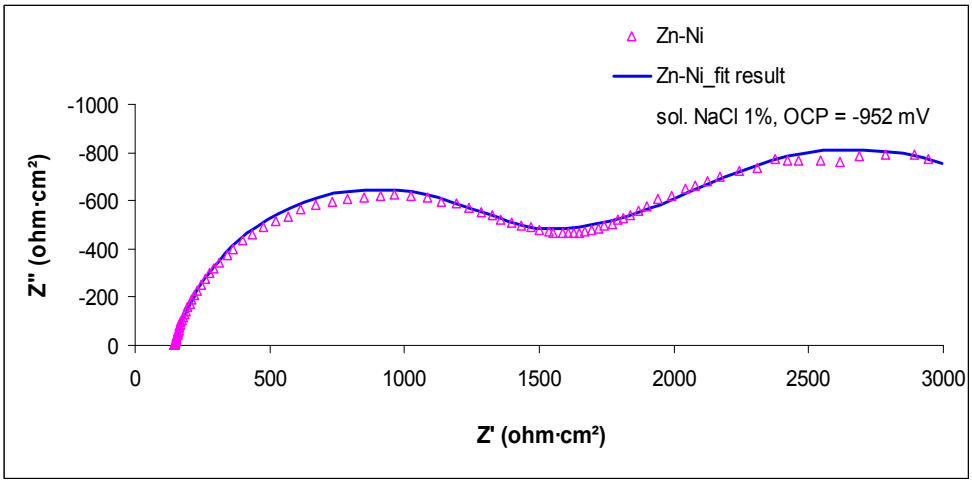

Figure 4. Nyquist diagrams for Zn-Ni alloy.

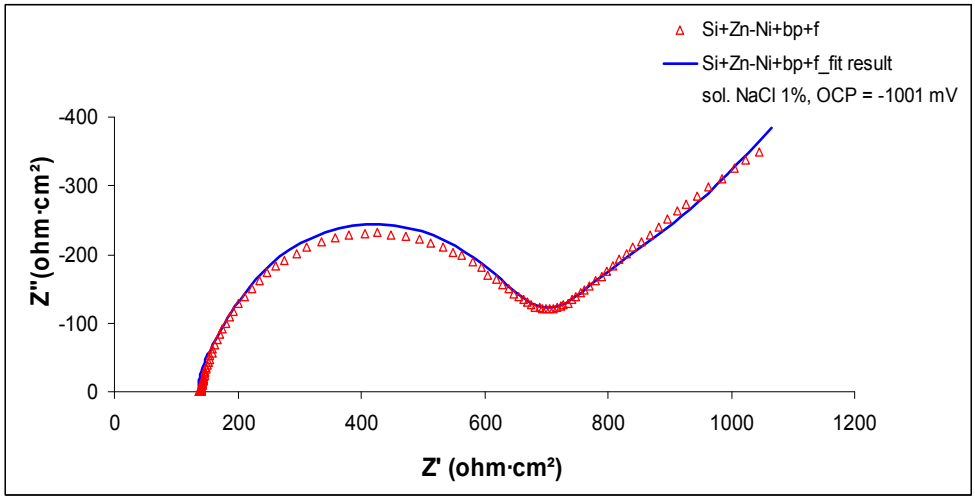

Figure 5. Nyquist diagrams for Zn-Ni alloy on steel/SiO_2.

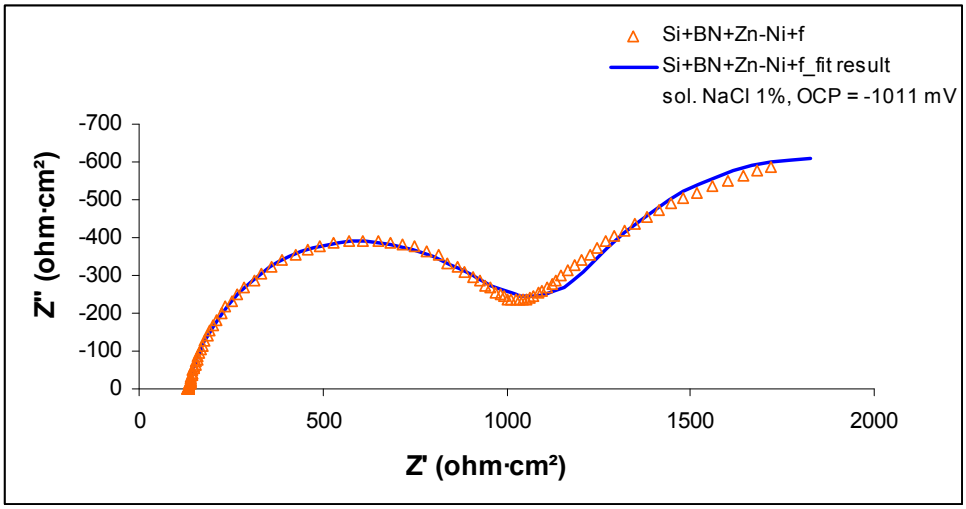

Figure 6. Nyquist diagrams for Zn-Ni alloy on steel/SiO_2/BN.

The correct interpretation of the electrochemical impedance spectra and the finding of a satisfactory equivalent circuit depend on a better understanding of corrosion phenomena at the sample surface. According to Suzuki [9] and Chung et al. [10], one of the cathode reactions on the zinc deposited sample surface in chloride ions environment, at intervals higher than -1.3 V (SCE) is the reduction of dissolved oxygen:

$$1/2O_2 + H_2O + 2e^- \rightarrow 2OH^-$$

This reaction increases the local pH at the surface of the zinc coating. The hydroxide film is the basis for further growth of corrosion products [10]. Corrosion products may consist of compounds such as ZnO, Zn $(OH)_2$, $ZnCO_3$, $ZN_5(OH)_6(CO_3)_2$ and $ZN_5(OH)_8Cl_2 \cdot H_2O$ and perhaps a mixture of these compounds [11]. Branco et al. [11] stated that due to their low solubility, the zinc corrosion products precipitate on the surface exposed to the action of sodium chloride solution. The film formed on the surface is not ideal and is not a completely compact layer, because the compactness of the film and the protective properties depend on the composition and formation conditions [9]. The pores in the corrosion products have influence on the electrochemical response of the system at low frequencies [9]. According to Yadav et al. [13] the stability of zinc corrosion products in chloride solutions depends on the concentration of $Cl^-$and H^+ ions as well as on the corrosion products, such as: $Zn(OH)_2$, $ZnCl_2 \cdot 6Zn(OH)_2$ and $ZnCl_2 \cdot 4Zn(OH)_2$ formed in chloride solutions [9.13]. The chemical reactions of this product are:

$$7ZnCl_2 \cdot 4Zn(OH)_2 + 4H_2O \rightarrow 5ZnCl_2 \cdot 6Zn(OH)_2 + 4H^+ + 4Cl^-$$
$$ZnCl_2 \cdot 6Zn(OH)_2 + 4H_2O \rightarrow 7Zn(OH)_2 + 2H^+ + 2Cl^-$$

These two reactions indicate that the chemical stability of corrosion products becomes larger with increasing concentrations of Cl^- and H^+ ions. According to Yadav et al. [13] the corrosion product $ZnCl_2 \bullet 4Zn(OH)_2$ formed at low pH has a porous structure. This porous corrosion product appears not to act as a barrier layer for O_2 and Zn^{2+} transport; thus corrosion continues. On the other hand, according to Giridhar and van Ooij [14] the increasing of the pH determines the passivation of the surface.

The equivalent circuit for the electrochemical impedance spectra corresponding to the samples steel/Zn-Ni, steel/SiO_2/Zn-Ni obtained in pulsed current and in magnetic field, as well as for steel/SiO_2/BN/Zn-Ni sample obtained in pulsed current, are shown in Figure 7. The equivalent circuit was mapped using ZView program.

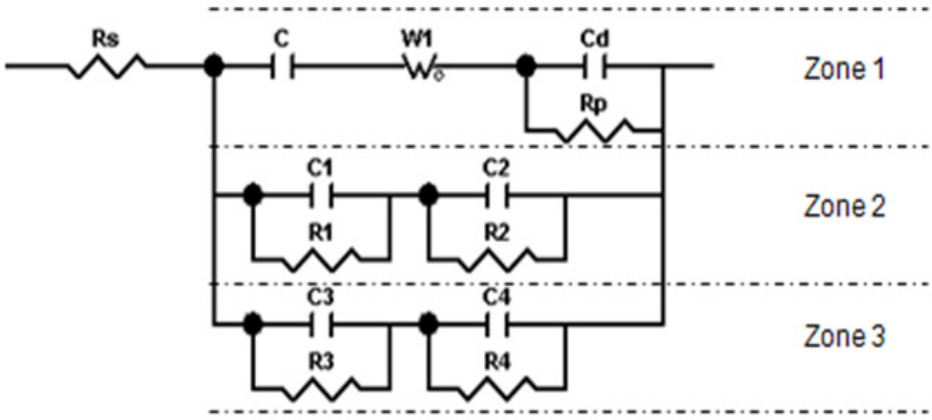

Figure 7. Equivalent circuit for Nyquist diagrams interpretation

On the surface of the studied sample there are three zones corresponding to the three levels (randomly distributed on the surface of the sample), showing different behaviors (figure 7).

Using the relation for the capacity of the plan capacitor ($C = \varepsilon_0\varepsilon_r S/d$) and the corresponding Warburg impedance relations ($W\text{-}T = L^2/D$) the thickness of the double electric layer (d_d), the thickness of the oxide layer ($d_1 + d_2$ and $d_3 + d_4$) and the length of diffusion (L_1) were determined as shown in Table 6.

Table 6. The double electric layer (d_d) diffusion length (L_1), the oxide layer formed in the second zone (d_1) thickness, the distance between the "fittings" of the capacitor formed by water molecules on oxide in the second zone (d_2), the oxide layer thickness formed in the third zone (d_3) and the distance between the "fittings" of the capacitor formed by the water molecules on oxide in the third zone (d_4).

Sample	d_d [Å]	L_1 [Å]	d_1 [Å]	d_2 [Å]	d_3 [Å]	d_4 [Å]
Zn-Ni	39.93	206	3	0.82	9.2	0.19
Si+ZnNi+bp+f	21.77	150	1.32	0.82	9.2	7.3
Si+B+ZnNi+f	41.12	651	3	0.82	9.2	0.19

From Table 6 it is observed that the thickness of the oxide layer (d_3 + d_4) formed on the sample Si + ZnNi + bp + f is approximately two times higher than the thickness of the oxide layer formed on the other samples.

Table 7. The values for the equivalent circuit elements (figure 7).

Equivalent circuit elements	Sample		
	Zn-Ni	Si+ZnNi+bp+f	Si+B+ZnNi+f
R_s [Ωcm^2]	39.33	35.41	35.83
R_p [Ωcm^2]	461.97	104.4	208.8
C_d [μF/cm^2]	17.88	32.79	17.36
R_1 [Ωcm^2]	991.8	652.5	730.8
C_1 [μF/cm^2]	8.81	20	8.81
R_2 [Ωcm^2]	1174.5	783	1174.5
C_2 [μF/cm^2]	862.4	862.4	862.4
R_3 [Ωcm^2]	1174.5	913.5	704.7
C_3 [μF/cm^2]	2.87	2.87	2.87
R_4 [Ωcm^2]	313.2	208.8	261
C_4 [μF/cm^2]	3620.6	3.62	3620.6

In Figure 8 is shown the schematic representation of the formations of the various oxide layers according to equivalent circuits presented in Figure 7.

From the data shown in tables 6 and 7 it can be assumed that for the sample obtained by conventional electrodeposition of Zn-Ni alloy on steel substrate, water molecules are adsorbed in the first zone on the surface (figure 8 a)) between the surface of the metal and the Helmholtz plane, which determines (from an electric point of view) the presence of a capacitance C. In the same zone, the diffusion of Zn^{2+} ions in the electrolyte is characterized (from electric point of view) by Warburg impedance (W_1). The presence of Zn^{2+}

ions in the electrolyte, near the surface, at a (d_d) distance, causes the formation of a capacitance (Cd) of the double electric layer and a polarization resistance (R_p). In the second zone (Figure 8 a)) a thin oxide layer is formed, with a (d_1) thickness, a (C_1) capacitance and a (R_1) resistance, and on this oxide layer a large numbers of water molecules are present (electric dipoles) that cause a (C_2) capacitance and a (R_2) polarization resistance. It was assumed that the dipoles concentration is high due to the high value of the (R_2) resistance. In the third zone (Figure 8) an oxide layer (d_3) is formed, thicker than in zone 2, having a (C_3) capacitance and a (R_3) resistance, followed by a dipolar layer of water molecules of (C_4) capacitance that causes a (R_4) polarization resistance.

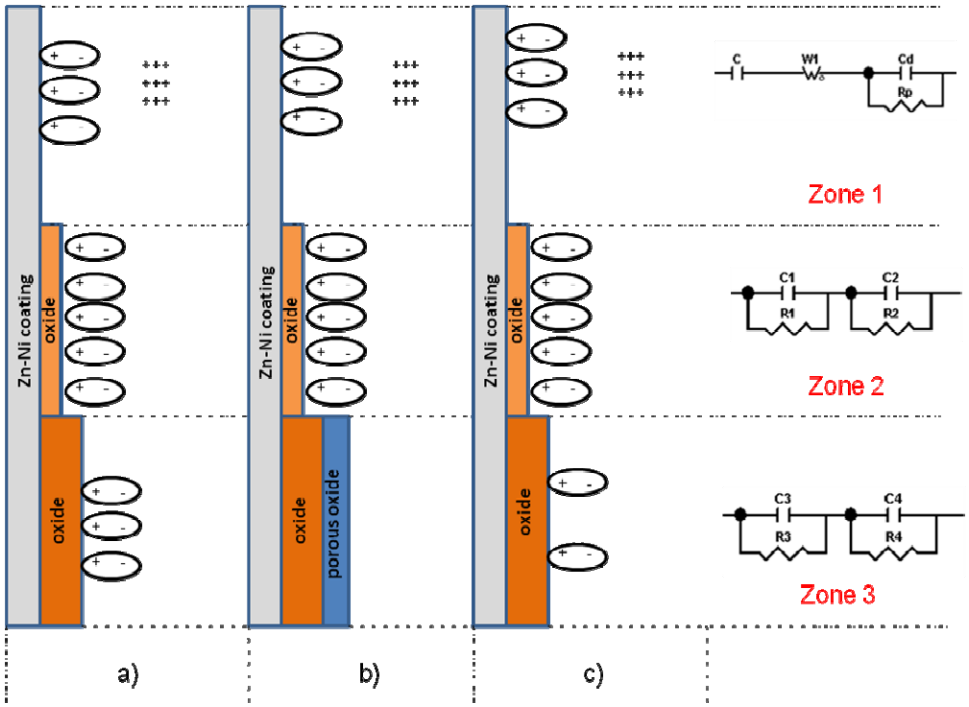

Figure 8. Schematic representation of the three zones and of the corresponding equivalent circuit for: a) the sample obtained by conventional electrodeposition of Zn-Ni alloy on steel substrate, b) the sample obtained by electrodeposition of Zn-Ni alloy in pulsed current and magnetic field on steel / silicon dioxide substrate (sample noted with Si + Zn-Ni + bp + f), c) the sample obtained by electrodeposition of Zn-Ni alloy in pulsed current on steel / silicon dioxide / boron nitride substrate (sample noted Si + B + Zn-Ni + f).

By analyzing the data for the sample obtained by electrodeposition of Zn-Ni alloy in pulsed current and magnetic field on steel / silicon dioxide substrate, shown in Tables 6 and 7, we can observe that the polarization resistance is lower than the polarization resistance of the sample obtained by conventional electrodeposition, and the thickness of the oxide layer formed in the second zone is lower (Figure 8 b)). In the third zone (Figure 8 b)) a (d_3) thickness oxide layer is formed on the surface, with a (R_3) resistance, and on this layer, a (d_4) thickness oxide layer is formed with a resistance three times lower than that of the base layer, which lead us to assume that this (d_4) thickness layer is porous.

From the data shown in tables 6 and 7, it can be observed that for the sample obtained by electrodeposition of Zn-Ni alloy in pulsed current on steel / silicon dioxide / boron nitride substrate, the polarization resistance is higher than that of the (Si + Zn-Ni + bp + f) sample, but is lower compared to that of the conventional electrodeposition. Generally, the sample obtained by electrodeposition of Zn-Ni alloy in pulsed current on steel / silicon dioxide / boron nitride substrate has a similar behavior with that of the sample obtained by conventional electrodeposition, but in the third zone (Figure 8 c)) it is observed that the (R_3) and (R_4) resistances are lower, which lead us to assume that the oxide layer formed is porous and the density of the dipoles on the surface is smaller.

The circuit formed by the C, W_1, C_d, R_p circuit elements, characterizes the corrosion active zones, the capacitance of the double electric layer, the polarization resistance and the diffusion. The circuit formed by the C_1, R_1, C_2, R_2 circuit elements, characterizes the zones where an oxide film is formed, followed by corrosion products zone. The circuit formed by the C_3, R_3, C_4, R_4 circuit elements characterizes the zones where an oxide layer is formed, followed by the formation of a porous oxide layer. The C_1, R_1, C_3, R_3 circuit elements are modeling the systems response at high frequencies, and the C_2, R_2, C_4, R_4 circuit elements are modeling the systems response at low frequencies

CONCLUSIONS

1. By comparing the results of potentiodynamic measurements and interpretation of Nyquist diagrams it can be concluded that the Zn-Ni alloy electrodeposited on steel / silicon dioxide (SiO_2) substrate in pulsed current and magnetic field and on steel / silicon dioxide (SiO_2) / boron nitride (BN) substrate in pulsed current show a better corrosion resistance compared to that of conventional electrodeposition on steel substrate.

2. According to the experimental data obtained for the three sets of samples it was found that for the same substrate, the samples corrosion resistance depends on the coating technique used. Also, for the same electrodeposition technique used, but for different substrates, the corrosion resistance is different. Thus, the corrosion resistance depends on the substrate and the coating technique used.

3. By comparing the results of potentiodynamic measurements and interpretation of Nyquist diagrams it can be concluded that the electrodeposited Zn-Ni alloy on steel / silicon dioxide (SiO_2) substrate in pulsed current and magnetic field shows the best protection against corrosion .

EXPERIMENTAL SECTION

Obtaining the samples

Experiments were carried out in the Corrosion and Corrosion Protection Laboratory of Technical University of Cluj-Napoca, Romania.

Substrate used for electrochemical deposition was commercially available rolled carbon steel sheet from which 16 cm^2 square samples were cut. All parts have been grinded with 1500 grit sandpaper. After grinding the pieces were degreased in 10% NaOH solution, washed, pickled in HCl solution (15%) and washed again.

To improve corrosion resistance, an intermediate layer was attempted which would have similar behavior with a diode so that the corrosion current would be as close to zero as possible.

For this purpose eight samples were immersed in sodium silicate (Na_2SiO_3) for 2 minutes, then 3 minutes in hydrochloric acid HCl (15%) solution in order to obtain a silicon dioxide (SiO_2) layer on the steel surface.

After being washed, four of the eight samples were covered with a boron nitride (BN) layer by electrodeposition, in order to obtain trivalent boron doped silicon. Electrochemical deposition of boron nitride was done with the sample mounted as anode and stainless steel was used as cathode [8].

In the end, the following substrates were obtained: steel (S235JR) steel / silicon dioxide (SiO_2) and steel / silicon dioxide (SiO_2) / boron nitride (BN). On these substrates a coating of ZnNi was electrodeposited by four methods: 1) conventional electrodeposition (Zn-Ni), 2) pulsed current electrodeposition (Zn-Ni + f), 3) electrodeposition in magnetic field with field lines parallel with the sample surface (Zn-Ni + bp), and 4) electrodeposition in pulsed current and magnetic field with field lines parallel with the sample surface (Zn-Ni + bp + f).

Electrolyte composition for Zn-Ni electrodeposition and for boron nitride (BN) is given in Tables 8 and 9.

Table 8. Bath composition for the Zn-Ni electrodeposition

Zincat	135,2 ml/l
NaOH	98 g/l
Performa Ni	12 ml/l
Performa BASE	6 ml/l
Performa BASE	94 ml/l
Performa BRI	2 ml/l
Performa ADD	0,7 ml/l
Current density	1,5 A/dm^2
Temperature	20-25 ^0C
Anodes	Nickel
Linear stirring of the cathode rod	10 oscillations/min

Table 9. Bath composition for the electrodeposition of boron nitride (BN)

H_3BO_3	100 g/l
$HCON(CH)_2$	100 g/l
Current density	1,5 mA/cm^2
Temperature	20-25 ^0C
Cathode	Stainless Steel
Distance anode - cathode	10 mm

Chemicals: Performa Ni, Performa BASE, Performa BRI and Performa ADD were purchased from the company COVENTYA S.A.S, France.

The electrodeposition in pulsed current was performed using a rectangular pulse generator with 25 ms pulse duration.

The magnetic field in which the samples were placed has a value of 70 mT and has the field lines parallel to the sample surface.

Corrosion testing

Potentiodynamic polarization testing

Potentiodynamic polarization tests were performed in order to determine the corrosion rate of Zn-Ni coatings. Corrosion tests were carried out using a Voltalab 10 potentiostat. The electrochemical cell consists of reference electrode (saturated calomel) platinum auxiliary electrode and work electrode which is the tested sample that has an area of 0.785 cm^2. The anode Tafel slope (βa), cathode slope (βc) and current density were determined at a potential scan rate of 10 mV/min, from +200 mV to -200 mV, against the open circuit potential.

Electrochemical impedance spectroscopy testing

The samples were placed in 1% NaCl solution during the electrochemical impedance spectroscopy (EIS) testing. The electrochemical cell consists of reference electrode (saturated calomel), platinum auxiliary electrode and the work electrode which is the tested

sample that has an area of 0.785 cm^2. Impedance data were obtained at open circuit potential using a Voltalab 10 potentiostat equipped with a frequency response analyzer. Impedance measurements were performed in a frequency range between 100 kHz and 1 mHz using a sinusoidal voltage with amplitude of 10 mV. Impedance spectra were analyzed using the attached software of the potentiostat.

ACKNOWLEDGMENT

This paper was supported by the project "Improvement of the doctoral studies quality in engineering science for development of the knowledge based society-QDOC" contract no. POSDRU/107/1.5/S/78534, project co-funded by the European Social Fund through the Sectorial Operational Program Human Resources 2007-2013.

REFERENCES

1. E. Popesco, R. Tournier, Zincarea electrolitică practică, Editura MEDRO, Bucureşti, **1998**.
2. Hwa Young Lee, Sung Gyu Kim, *Surface and Coatings Technology*, **2000**, *135*, 69.
3. G. Barcelo, *Journal of Applied Electrochemistry*, **1998**, *28*,1113.
4. Brenner, Electrodeposition of Alloys: Principles and Practice, Vols. I and II, Academic Press, New York, **1963**.
5. E. Gomez, *Metal Finishing*, **1991**, *6*, 44.
6. S. Couchane, J Douglade, J. Amblard, R. Rehamnia, J.-P. Chopart, Metal field effects on Zn-Ni electrodeposition, the 15thRiga and 6th PAMIR Conference on Fundamental and Applied MHD. **2005**.
7. T. Frade, V. Bouzon, A. Gomes, M.I. Pereira da Silva, *Surface and Coatings Technology*, **2010**, *204*, 3592.
8. M. Pal Chowdhurya, B.R. Chakrabortyb, A.K. Pal, *Materials Letters*, **2004**, 58, 3362 Suzuki, *Corrosion Science*, **1985**, *25*, 1029.
9. S.C. Chunga, J.R. Chengb, S.D. Chioub, H.C. Shiha, *Corrosion Science*, **2000**, *42*, 1249.
10. V. Barranco, S. Feliu Jr., S. Feliu, *Corrosion Science*, **2004**, *46*, 2203.
11. R.G. Kelly, J.R. Scully, D.W. Shoesmith, R.G. Buchheit, *Electrochemical Techniques in Corrosion Science and Engineering*, first ed., Marcel Dekker, Inc., New York, **2003**, pp. 205–255.
12. A.P. Yadav, A. Nishikata, T. Tsuru, *Corrosion Science*, **2004**, *46*, 361.
13. Giridhar, W.J. van Ooij, *Surface & Coatings Technology*,**1992**, *53*, 35.
14. V.R. Rao, V. Kasturi, H. Chitharanjan, *Journal of Magnetism and Magnetic Materials*, **2013**, *345*, 48.
15. K.R. Sriraman, S. Brahimi, J.A. Szpunar, J.H. Osborne, S. Yue, *Electrochimica Acta*, **2013**, *105*, 314.